

# General Oscillator-Based Ising Machine Models with Phase-Amplitude Dynamics and Polynomial Interactions

Lianlong Sun,<sup>\*</sup> Matthew X. Burns,<sup>†</sup> and Michael C. Huang<sup>‡</sup>  
*Department of Electrical and Computer Engineering, University of Rochester, USA*

We present an oscillator model with both phase and amplitude dynamics for oscillator-based Ising machines (OIMs). The model targets combinatorial optimization problems with polynomial cost functions of arbitrary order and addresses fundamental limitations of previous OIM models through a mathematically rigorous formulation with a well-defined energy function and corresponding dynamics. The model demonstrates monotonic energy decrease and reliable convergence to low-energy states. Empirical evaluations on 3-SAT problems show significant performance improvements over existing phase-amplitude models. Additionally, we propose a flexible, generalizable framework for designing higher-order oscillator interactions, from which we derive a practical method for oscillator binarization without compromising performance. This work strengthens both the theoretical foundation and practical applicability of oscillator-based Ising machines for complex optimization problems.

## I. INTRODUCTION

The limitations of traditional von Neumann architectures in efficiently tackling combinatorial optimization problems have spurred the exploration of alternative computing paradigms. Among these, Ising machines, inspired by the Ising model from statistical mechanics, have emerged as a promising approach. The versatility of Ising machines extends across a diverse range of applications, including portfolio optimization [1, 2], drug discovery [3], vehicle routing [4–6], fraud detection [7], clustering [8], power grid optimization [9], wireless communication [10, 11], image restoration [12] and machine learning [13–17]. Additionally, Ising machines leverage multiple specialized hardware substrates, including quantum [18, 19], optical [20–29], CMOS [30–37] and other emerging hardware platforms [38–44]. By mapping the decision variables of an optimization problem onto interacting spins [45], Ising machines can efficiently search for solutions by allowing the system to naturally evolve towards its lowest energy state. This process corresponds to finding a configuration of spins that minimizes the system’s energy, which directly translates to a high-quality solution to the original optimization problem. This approach offers the potential to significantly accelerate the solution of complex optimization problems that are intractable for classical computers.

A major challenge in Ising machine implementations is that the original Ising model supports only up to second-order interactions. Mapping practical problems such as 3-SAT introduces third-order terms into the Hamiltonian, creating a fundamental mismatch between the problem structure and the physical implementation. A widely adopted approach to address this issue is cubic-to-quadratic reduction [46–49], which introduces auxiliary variables. However, this method often complicates the energy landscape, making it more difficult to navigate [50], and consequently leads to suboptimal performance [51, 52]. Recent advances [51–54] have proposed

native supports for higher-order interactions, avoiding the need for any reductions.

Ising machines based on networks implementing the Kuramoto model [55] of synchronization have gained significant traction. These oscillator-based Ising machines (OIMs) [56–67] based on Kuramoto model exploit the emergent collective behavior of synchronized oscillators to emulate spin interactions, with the system’s natural tendency towards stable, synchronized states corresponding to low-energy solutions of the Ising Hamiltonian. While Kuramoto-based OIMs have shown promise, oscillator models that incorporate amplitude dynamics in addition to phase [51, 68–71] have aimed to provide a more complete physical description of the underlying hardware. Research has revealed that phase-amplitude formulations for nanoelectromechanical (NEMS) oscillators can diverge significantly from simplified phase-only descriptions under specific operating regimes [68]. Moreover, incorporating amplitude dynamics into spintronic oscillator models (Slavin’s model [69]) yields a more faithful representation of coupled magnetization processes and the system demonstrates improved time complexity over the Goemans-Williamson algorithm [71]. For consistency with [51], we refer to models that integrate both amplitude and phase in the context of Ising machines as the *Hopf oscillator model*.

Our study is motivated by the need for a faithful, general oscillator model that incorporates both phase and amplitude dynamics while supporting higher-order interactions. We begin by identifying critical limitations in the previously proposed Hopf oscillator model for optimization problems [51]:

- **Lack of a Physically Meaningful Hamiltonian Definition:** A central concept in Ising machines is the system’s energy, which should correspond to the objective function being optimized. In previous work, the defined energy function is generally complex-valued, lacking a clear physical interpretation. This contrasts with traditional Ising machines where energy is a real-valued function directly related to the optimization problem cost function.
- **Non-Monotonic Energy Decrease:** Ideally, the system’s energy should be able to decrease monotonically in the absence of introduced noise. In prior model [51], we

<sup>\*</sup> Contact author: lianlongsun@rochester.edu

<sup>†</sup> Contact author: mburns13@ur.rochester.edu

<sup>‡</sup> Contact author: michael.huang@rochester.edu

observed that neither individual parts (real or imaginary) nor absolute value of the energy consistently decrease during the optimization process.

To address these limitations, we have developed an oscillator model with complex-valued oscillator representation, based on Andronov-Hopf dynamics [72], providing a rigorous framework for oscillator-based Ising machines. Our key contributions include:

- **Energy Definition:** We introduce the complex conjugate of the oscillator representation variable  $z$  to define a real-valued and physically meaningful energy function that directly corresponds to the objective function of the optimization problem.
- **Oscillator Dynamics Derivation:** Using Wirtinger calculus [73], we derive the oscillator dynamics from our redefined energy function. These dynamics guarantee a monotonic decrease in energy under ideal conditions as the system evolves towards a solution.
- **Generalization to Higher-Order Interactions:** Our formulation naturally extends higher-order interactions among oscillators, thus broadening its applicability to more complex optimization problems.
- **Alternative Binarization Approach:** We propose an alternative method for binarizing the oscillator variable  $z$ , derived from the model formulation. This approach maintains solution quality while providing flexibility in implementation.

This rigorous framework not only provides a deeper theoretical understanding of OIMs but also leads to significant empirical performance improvements compared to existing phase-amplitude approaches. Remarkably, the energy function terms in our model closely resemble those found in nonlinear optical or four-wave mixing Hamiltonian [74, 75]. This connection suggests exciting new paths for realizing powerful Ising machines, potentially leveraging existing photonic technologies. Furthermore, we demonstrate that our model reduces to a previously proposed high-order, Kuramoto-based formulation [54] once amplitude dynamics are removed. Our work therefore generalizes previous polynomial frameworks, offering perspective on the relationship between Hopf and Kuramoto oscillator models for Ising machines.

Our findings offer a stronger theoretical foundation for OIMs while providing actionable guidelines for leveraging their potential to address complex optimization challenges.

## II. BACKGROUND AND PRELIMINARIES

### A. Ising Hamiltonian for Combinatorial Optimization

1-D spin glass systems were originally proposed as a model for quenched disorder and frustration in metallic alloys [76, 77]. For  $N$  1-D spins  $s = (s_1, \dots, s_N)$  with a coupling matrix  $J \in \mathbb{R}^{N \times N}$  and external bias  $h \in \mathbb{R}^N$ , the Ising spin glass

(ISG) Hamiltonian, named after Ernst Ising for his earlier work on purely ferromagnetic systems [78], is given by

$$H(s) = - \sum_{i < j} J_{ij} s_i s_j - \sum_{i=1}^N h_i s_i. \quad (1)$$

Later work revealed that finding the ground state of a spin glass is NP-hard [79, 80]. Accordingly, a number of high-impact combinatorial problems can be mapped to an equivalent spin glass system [45, 81]. In particular, an ISG Hamiltonian can be trivially mapped to Quadratic Unconstrained Binary Optimization (QUBO) problems, a well-studied class within operations research [82].

The relative simplicity of the ISG Hamiltonian makes it highly amenable for hardware acceleration, leading to the advent of “Ising machines” (IMs) [81]: devices which “implement” the Ising Hamiltonian in some manner. IM proposals include purely digital accelerators [83, 84], analog devices evolving a continuous relaxation of the Ising Hamiltonian [35, 56, 85], and hybrid digital/analog systems [86, 87].

### B. Solving 3-SAT problems with Ising Machine

Ising machines have been successfully applied to quadratic unconstrained binary optimization (QUBO) problems [35, 56, 88] and even polynomial unconstrained binary optimization (PUBO) [51, 54, 89] problems with the help of higher-order interactions. A generic Ising machine workflow usually involves ① converting the problem to a discrete Ising formula, ② mapping the formula to a continuous-time, dynamical Ising machine capable of seeking the minimum energy state and ③ extracting the solution from the final device state. In this subsection, we demonstrate how to map 3-SAT problems to an Ising Machine as a preliminary step.

Consider a Boolean formula  $f : \{0, 1\}^N \rightarrow \{0, 1\}$  in 3-literal conjunctive normal form (3-CNF)

$$f(x) = \bigwedge_{j=1}^m (\ell_{j,1} \vee \ell_{j,2} \vee \ell_{j,3}), \quad (2)$$

where each  $\ell_{j,1}$  is a *literal* (either a variable  $x_p$  or its negation  $\bar{x}_p$ ) and each disjunction of literals  $(\ell_{j,1} \vee \ell_{j,2} \vee \ell_{j,3})$  is a *clause*. The 3-SAT problem consists of finding some  $x$  such that  $f(x) = 1$ , i.e., an assignment satisfying all of the clauses. We restrict ourselves to 3-SAT without loss of generality, as any  $K$ -SAT problem can be reduced to an equivalent 3-SAT problem by adding  $O(K \cdot m)$  variables and clauses [90].

Let  $s = \{s_i\}_{i=1}^n \in \{-1, +1\}^n$  be the vector of Ising spins. We follow the standard convention that  $s_i = 1 \iff x_i = 1$  and  $s_i = -1 \iff x_i = 0$  [45].

For each literal  $\ell_{j,k} \in \{x_p, \bar{x}_p\}$  we define a spin function  $L_{j,k} : \{-1, 1\}^n \rightarrow \{0, 1\}$  as

$$L_{j,k}(s) = \frac{1}{2} \begin{cases} 1 - s_p & \text{if } \ell_{j,k} = x_p \\ 1 + s_p & \text{if } \ell_{j,k} = \bar{x}_p \end{cases}, \quad (3)$$

where  $L_{j,k}(s) = 0$  if the literal is satisfied, and 1 otherwise.

A clause  $c_j = (\ell_{j,1} \vee \ell_{j,2} \vee \ell_{j,3})$  is satisfied if at least one of its literals is true. Similarly to individual literals, we can define a spin function  $C_j(s)$  as

$$C_j(s) = L_{j,1}(s) \cdot L_{j,2}(s) \cdot L_{j,3}(s), \quad (4)$$

where  $C_j(s) = 0$  if  $c_j$  is satisfied and 1 otherwise.

Substituting Eq. 3, we can see that each  $C_j$  is a spin polynomial of degree three

$$C_j(s) = \left( \frac{1 \pm s_p}{2} \right) \left( \frac{1 \pm s_q}{2} \right) \left( \frac{1 \pm s_r}{2} \right), \quad (5)$$

where  $s_p$ ,  $s_q$ , and  $s_r$  are spins corresponding to the variables of each literal.

We then define the objective function  $E : \{-1, 1\}^N \rightarrow \mathbb{Z}_+$  as the sum of all clause functions  $C_j(s)$ ,

$$E(s) = \sum_j C_j(s) = \sum_j L_{j,1}(s) L_{j,2}(s) L_{j,3}(s). \quad (6)$$

From Eq. 5, when a clause is satisfied, its corresponding  $C_j$  evaluates to zero, contributing nothing to the total energy. In contrast, if a clause is unsatisfied,  $C_j$  contributes a positive value of 1 to  $\mathcal{H}$ . Therefore, minimizing  $\mathcal{H}$  effectively minimizes the number of unsatisfied clauses. The optimization problem can thus be formally stated as

$$E = \sum_{i=1}^n h_i s_i + \sum_{i=1}^n \sum_{j=1}^n J_{ij} s_i s_j + \sum_{i=1}^n \sum_{j=1}^n \sum_{k=1}^n P_{ijk} s_i s_j s_k + \text{constant}, \quad (7)$$

where  $h$ ,  $J$ , and  $P$  are the coefficient vector, the coupling matrix, and the three-body interaction tensor, respectively. Minimizing  $E$  corresponds to finding an assignment of spin variables  $s_i$  that satisfies the maximum number of clauses. A solution with  $E = 0$  indicates that all clauses are satisfied, thereby providing a solution to the original 3-SAT problem. Appendix A provides a concrete example by mapping a single 3-SAT clause to the PUBO Hamiltonian.

In practice, analog Ising machines often represent binary spins  $s$  by some physical quantities, thus relaxing the discrete phase space into a continuous one. We assume native device support for 3-body interactions and focus on the performance of the specific formulation. 3-body interactions can be implemented in analog electronic systems by means of multi-input gates (see [52, 54] for more details).

### C. Kuramoto Oscillator Model

The Kuramoto model [55] was originally proposed as a phase reduction method to study synchronization phenomena in weakly-coupled oscillator networks [91, 92]. A system of  $N$  coupled oscillators with phase  $\theta = (\theta_1, \dots, \theta_N)$  is described by a system of coupled ODEs

$$\frac{d\theta_i}{dt} = \kappa \sum_{\substack{j=1 \\ j \neq i}}^N J_{ij} \sin(\theta_i - \theta_j) + \omega_i, \quad (8)$$

where  $\kappa$  and  $J_{ij}$  describe global and pairwise interaction strengths respectively, and  $\omega_i$  is the natural frequency of the  $i^{\text{th}}$  oscillator. We set  $\omega_i = 0$  in Eq. 8 assuming that all oscillators have identical  $\omega_i$  and viewing the system in a rotating reference frame. Using spin glass interaction coefficients for  $J$  has led to oscillator-based accelerators for combinatorial optimization: *oscillator Ising machines* (OIM) [56–66, 93, 94].

We can trivially derive the global Lyapunov function associated with Eq. 8 as

$$E(\theta) = \kappa \sum_{i < j} J_{ij} \cos(\theta_i - \theta_j). \quad (9)$$

The coupled oscillator system tends to minimize energy  $E(\theta)$  over time [95], laying the foundation for OIMs that tackle combinatorial optimization problems. The original OIM architecture [56] utilized electronic LC-tank oscillators, and more recent proposals have broadened the choice of substrate to ring oscillators [96, 97], phase transition nano-oscillators [98–100], and magnetic tunnel junctions [101, 102].

### D. Sub-harmonic Injection Locking

The key idea of an OIM (and analog Ising machines in general) is to evolve the system towards a lower energy state, then map the state back to ISG spins. We term the mapping from oscillator's XY spin state (0 to  $2\pi$  in phase) to Ising spins (0 or  $\pi$ ) as *binarization*. However, the stationary points of the oscillator system may not have a known binarization. For instance, a two-oscillator system  $H(\theta) = \cos(\theta_1 - \theta_2)$  has infinitely many stationary points of the form

$$\theta_1 - \theta_2 = \pi. \quad (10)$$

For a toy 2-oscillator system, the binarization is clear. However, coupled Kuramoto oscillator networks may not permit a closed-form binarization scheme. Kuramoto synchronization results in the oscillators bifurcating to aligned/non-aligned phases along some axis in the imaginary plane; however, that axis is not known a priori. To provide a simple, bijective mapping between oscillator fixed points and spin states, techniques such as sub-harmonic injection locking (SHIL) are introduced.

To provide simple binarization, previous work [56] injects a sub-harmonic injection locking (SHIL) term into their spin dynamics,

$$\frac{d\theta_i}{dt} = \kappa \sum_{i < j}^N J_{ij} \sin(\theta_i - \theta_j) - \kappa_S(t) \overbrace{\sin(2\theta_i)}^{\text{SHIL}}. \quad (11)$$

The second harmonic creates a potential well at  $\theta_i = n\pi$  for  $n \in \mathbb{N}$ , inducing sub-harmonic injection locking (SHIL). During annealing, periodic application of SHIL forces the oscillators to bifurcate, with appropriate hyperparameters ensuring a final two-cluster bifurcation.

### III. METHODS

#### A. Hopf Oscillator Model

While the Kuramoto model is sufficient to study phase-only phenomena, real-world oscillators will have variability in both phase and amplitude. To enable a more faithful model, we can generalize from the phase-reduced representation to complex  $z \in \mathbb{C}^N$ . An oscillator model for combinatorial optimization and sampling is the Adronov-Hopf model (or ‘‘Hopf model’’ for brevity) [51, 72]. The evolution of each Hopf oscillator is given by a system of coupled ODEs

$$\frac{dz_i}{dt} = f(z_i) + g(z), \quad (12)$$

where  $z_i$  describes the phase and amplitude of the  $i$ -th oscillator,  $f(z_i)$  represents the local dynamics of the oscillator, and  $g(z)$  represents the coupling interaction between oscillators. In previous work [51] (which is also the baseline we compare with), the local dynamics  $f(z_i)$  is defined as

$$f(z_i) = (\lambda_i + i\omega_i)z_i + \rho_i z_i |z_i|^2, \quad (13)$$

where the center frequency is set to  $\omega_i = 0$  for all oscillators. The parameters  $\lambda_i$  and  $\rho_i$  are chosen such that the system exhibits a stable limit cycle with unit amplitude. The term  $g(z)$  is derived from the model energy function  $\mathcal{H}$ . Previous work [51] directly maps the optimization problem to the system energy function  $\mathcal{H}$  by replacing the Ising spin variable  $s_i$  in Eq. 7 with the complex oscillator representation  $z_i$  as follows:

$$\begin{aligned} \mathcal{H} = & \sum_{i=1}^n h_i z_i + \sum_{i=1}^n \sum_{j=1}^n J_{ij} z_i z_j \\ & + \sum_{i=1}^n \sum_{j=1}^n \sum_{k=1}^n P_{ijk} z_i z_j z_k + \text{constant}. \end{aligned} \quad (14)$$

Several observations motivate us to investigate a new formulation:

1. The energy  $\mathcal{H}(z)$  is generally complex-valued. While the function is holomorphic and mathematically differentiable, the physical interpretation of a complex energy remains ambiguous.
2. The model does not ensure that the real part, imaginary part, or absolute value of  $\mathcal{H}(z)$  decreases monotonically under ideal conditions. This raises concerns about convergence and optimization efficiency. Lyapunov stability analysis, typically used to demonstrate that a system seeks a local minimum of an energy function, is not applicable here.

To address the challenges in accurately describing the system and the oscillator dynamics with a complex variable  $z_i$ ,

1. We introduce the complex conjugate  $z_i^*$  into the energy function. This approach enables the formulation of a real-valued energy function  $\mathcal{H}'(z)$  that provides a meaningful physical interpretation of the system.

2. Using the new energy function, we derive system dynamics using gradient of the energy function. The resulting gradient system naturally drives the state toward minima of the real-valued energy function.

Specifically, one of the energy functions of our Hopf oscillator model is defined as follows:

$$\begin{aligned} \mathcal{H}' = & \frac{1}{2} \sum_{i=1}^n h_i (z_i + z_i^*) + \sum_{i=1}^n \sum_{j=1}^n J_{ij} z_i z_j^* \\ & + \frac{1}{2} \left( \sum_{i=1}^n \sum_{j=1}^n \sum_{k=1}^n P_{ijk} z_i z_j z_k^* \right. \\ & \left. + \sum_{i=1}^n \sum_{j=1}^n \sum_{k=1}^n P_{ijk} z_i z_j^* z_k^* \right) + \text{constant}. \end{aligned} \quad (15)$$

Note that this construction is not unique; in Sec. IV B we discuss a general framework for generating appropriate energy functions.

With the introduction of the complex conjugate, the energy function is no longer holomorphic. However, by applying Wirtinger calculus [73], we can rigorously derive the system dynamics. The core idea of Wirtinger calculus is to treat the complex function  $f(z)$  as a function of both  $z$  and its conjugate  $z^*$  as independent variables. For non-holomorphic functions, this requires differentiation with respect to both variables. Appendix B contains a brief overview of Wirtinger calculus.

The symmetry of our energy functions with respect to  $z$  and  $z^*$  permits a simplification: we can compute the gradient by considering only the derivative with respect to either  $z$  or  $z^*$ . Now we have,

$$\begin{aligned} \frac{\partial \mathcal{H}'}{\partial z_i} = & \frac{1}{2} h_i + \sum_{j=1}^n J_{ij} z_j^* \\ & + \frac{1}{2} \left( \sum_{j=1}^n \sum_{k=1}^n P_{ijk} z_j z_k^* + \sum_{i=1}^n \sum_{k=1}^n P_{ijk} z_i z_k^* \right. \\ & \left. + \sum_{j=1}^n \sum_{k=1}^n P_{ijk} z_j^* z_k^* \right). \end{aligned} \quad (16)$$

For convenience, the coefficient  $P$  is constructed to be symmetric under all permutations of its indices. It follows that  $\sum_{j=1}^n \sum_{k=1}^n P_{ijk} z_j z_k^* = \sum_{i=1}^n \sum_{k=1}^n P_{ijk} z_i z_k^*$ . Therefore, summing over any two of the three indices yields the same result. To drive the system towards minimizing the energy, we set

$$\frac{dz_i}{dt} = - \left( \frac{\partial \mathcal{H}'}{\partial z_i} \right)^*. \quad (17)$$

Furthermore, we have the identity

$$\frac{dz_i}{dt} = \left( \frac{dz_i^*}{dt} \right)^*, \quad (18)$$

which follows from the definition of  $z$  and  $z^*$ . Additionally, we have

$$\left(\frac{\partial \mathcal{H}'}{\partial z_i}\right)^* = \frac{\partial \mathcal{H}'}{\partial z_i^*}, \quad (19)$$

which follows from the conjugation property of Wirtinger derivatives (see Appendix B). Combining these results with Eq. 17, we obtain the total derivative:

$$\begin{aligned} \frac{d\mathcal{H}'}{dt} &= \sum_i \frac{\partial \mathcal{H}'}{\partial z_i} \frac{dz_i}{dt} + \sum_i \frac{\partial \mathcal{H}'}{\partial z_i^*} \frac{dz_i^*}{dt} \\ &= -2 \sum_i \frac{\partial \mathcal{H}'}{\partial z_i} \left(\frac{\partial \mathcal{H}'}{\partial z_i}\right)^* \\ &= -2 \sum_i \left[ \text{Re} \left(\frac{\partial \mathcal{H}'}{\partial z_i}\right)^2 + \text{Im} \left(\frac{\partial \mathcal{H}'}{\partial z_i}\right)^2 \right] \leq 0, \end{aligned} \quad (20)$$

with equality if and only if  $\frac{d\mathcal{H}'}{dz_i} = 0$ , i.e., at a stationary point. Since the Hessian operator remains continuous in Wirtinger calculus [73], the dynamics (Eq. 20) are locally Lyapunov stable within some neighborhood for all minima. Therefore, Eq. 15 is a suitable Lyapunov function for complex-domain Ising machines. In contrast, the energy formulation proposed in previous work [51] is complex-valued and cannot serve as a viable Lyapunov function<sup>1</sup>.

## B. Compatibility with Kuramoto model

The Kuramoto model was originally derived as a phase reduction for networks of weakly coupled oscillators [55]. Both the phase-only model (including the quadratic Kuramoto model) and the Hopf model only approximate real-world oscillators. However, the Hopf model is more expressive, as it accounts for amplitude variations. One would expect that in the case of amplitude homogeneity, the Hopf model reduces to the phase-only model. Here, we show that indeed the Hamiltonian of our model, Eq. 15 can be used to derive phase-only models found in previous literature in the context of cubic forms. In so doing, we demonstrate our model ① conforms to physical intuition and ② generalizes previous work.

<sup>1</sup> Disregarding the physical interpretation of the complex-valued  $\mathcal{H}$ , we examine the behavior of the baseline model [51] on a simple 3-variable problem,  $E = s_1 s_2 s_3$ , where  $s_i \in \{-1, +1\}$ . Both real and imaginary components exhibit oscillatory behavior, which leads to unstable dynamics. This can be demonstrated mathematically and empirically, and the observation extends to general cases.

Expressing  $z_i = |z_i|e^{-i\theta_i}$ , we have the equivalent expression

$$\begin{aligned} \mathcal{H}'(z) &= \frac{1}{2} \sum_{i=1}^n h_i |z_i| (e^{i\theta_i} + e^{-i\theta_i}) \\ &+ \sum_{i=1}^n \sum_{j=1}^n J_{ij} |z_i| |z_j| e^{i(\theta_i - \theta_j)} \\ &+ \frac{1}{2} \left( \sum_{i=1}^n \sum_{j=1}^n \sum_{k=1}^n P_{ijk} |z_i| |z_j| |z_k| e^{i(\theta_i + \theta_j - \theta_k)} \right) \\ &+ \sum_{i=1}^n \sum_{j=1}^n \sum_{k=1}^n P_{ijk} |z_i| |z_j| |z_k| e^{-i(\theta_i + \theta_j - \theta_k)} \\ &+ \text{constant}. \end{aligned} \quad (21)$$

Since  $\mathcal{H}'(z)$  is real by construction, we have

$$\begin{aligned} \mathcal{H}'(z) &= \text{Re}[\mathcal{H}'(z)] \\ &= \sum_{i=1}^n h_i |z_i| \cos(\theta_i) \\ &+ \sum_{i=1}^n \sum_{j=1}^n J_{ij} |z_i| |z_j| \cos(\theta_i - \theta_j) \\ &+ \sum_{i=1}^n \sum_{j=1}^n \sum_{k=1}^n P_{ijk} |z_i| |z_j| |z_k| \cos(\theta_i + \theta_j - \theta_k) \\ &+ \text{constant}. \end{aligned} \quad (22)$$

If we further assume amplitude homogeneity ( $|z_i| = |z_j| = |z_k| = 1$ ), which will remove the amplitude dynamics from the model, then we obtain

$$\begin{aligned} \mathcal{H}'(z) &= \sum_{i=1}^n h_i \cos(\theta_i) + \sum_{i=1}^n \sum_{j=1}^n J_{ij} \cos(\theta_i - \theta_j) \\ &+ \sum_{i=1}^n \sum_{j=1}^n \sum_{k=1}^n P_{ijk} \cos(\theta_i + \theta_j - \theta_k) + \text{constant}, \end{aligned} \quad (23)$$

which is identical to the form proposed in Ref. [54].

## IV. Results

### A. Model Evaluation

We compare our proposed Hamiltonian (Eq. 15) against the previously established baseline [51] (Eq. 14), which also incorporates the amplitude dynamics for oscillator-based Ising machines. We simulate these models by numerically solving their governing differential equations.

**Overall Performance:** We evaluate model performance on 1,700 uniform random 3-SAT benchmarks from SATLIB [103]. Each set, `ufN-M`, denotes instances with  $N$  variables and  $M$  clauses; we use `uf20-91`, `uf50-218`, `uf75-325`, `uf100-430`, and `uf150-645`, all at a clause-to-variable ratio of approximately 4.3. This ratio lies at the empirical *phase*

*transition* in satisfiability, where random 3-SAT instances shift from mostly satisfiable to mostly unsatisfiable and where difficulty peaks [104]. We define a *solvable instance* as one where at least one of 100 independent runs (with different initial conditions) reaches zero energy within a sufficient simulation time ( $T = 136$ ), allowing both models to achieve their best performance on the benchmark.

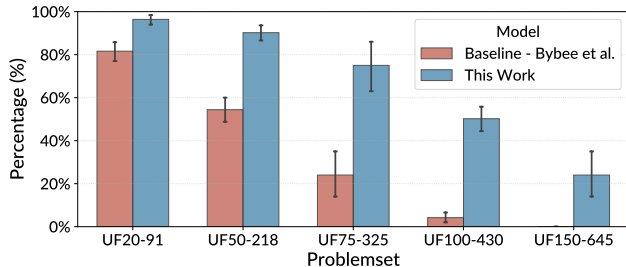


FIG. 1. Percentage of solvable instances across problem sets (UF20-91 to UF150-645) from SATLIB [103] under 100 runs per instance. Instances are classified as *solvable* if at least one run reaches the ground state ( $\mathcal{H} = 0$ ). The error bars denote the 99% bootstrap confidence intervals (computed over 10,000 resamples). The proposed Hopf model consistently outperforms the baseline model [51].

The following results show that our approach consistently outperforms the baseline Hopf model: We solve a higher percentage of instances and achieve lower final energy values more frequently. These improvements indicate superior optimization performance, as illustrated in Fig. 1 and Fig. 2.

### B. Higher-order Models with Wirtinger Potentials

For effective optimization of combinatorial problems and accurate representation of the Ising formulation, the energy function of an oscillator system ideally satisfies two key conditions:

1. It should establish a clear correspondence between the continuous system energy and the original optimization problem. One approach to achieve this is through a real-valued energy function.
2. Upon binarization, the energy function would optimally yield the same values as the discrete Ising formulation. For instance, with a complex oscillator representation  $z$ , one may map  $\text{Re}(z_i) > 0$  to  $s_i = +1$  and  $\text{Re}(z_i) < 0$  to  $s_i = -1$ ; alternatively, in a phase-only model, upon binarization, mapping  $\phi_i = 0$  to  $s_i = +1$  and  $\phi_i = \pi$  to  $s_i = -1$  achieves this equivalence.

There are multiple ways to construct an energy function that satisfies these conditions. The most natural approach is to replace spin  $s_i$  with  $\frac{z_i + z_i^*}{2|z_i|}$ . The resulting cubic terms of an energy function (ignoring the constant factor) will be

$$\mathcal{H}_3^C(z) = \sum_{i,j,k} (z_i + z_i^*) (z_j + z_j^*) (z_k + z_k^*). \quad (24)$$

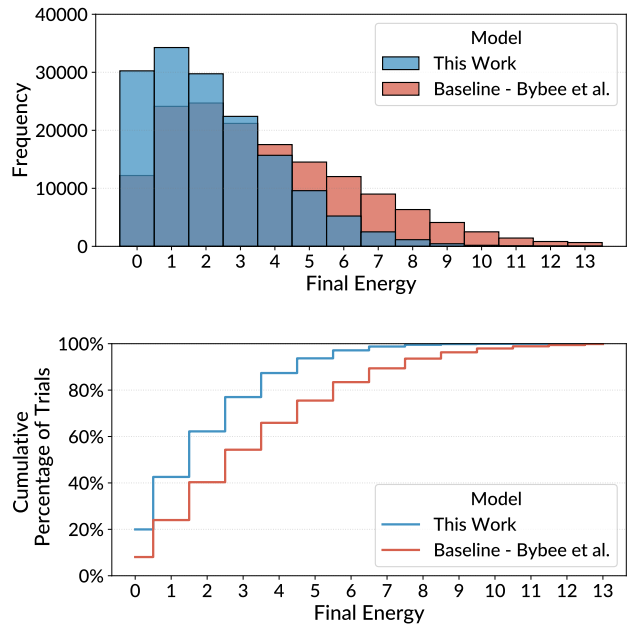


FIG. 2. Final energy distribution for solving 3-SAT problems across approximately 170,000 runs per model. The proposed Hopf model achieves lower final energies with higher frequency, as shown in the histogram (top). The cumulative plot (bottom) further demonstrates the improved performance, showing a higher percentage of trials for the proposed model successfully reaching optimal or near-optimal solutions.

We refer to this as the *Complete potential* (or C-potential for short) for cubic interactions, as it involves a complete set of cross terms. However, a family of systematic subsets of its terms can each satisfy the desired conditions. Taking cubic terms as an example:

$$\begin{aligned} \mathcal{H}_3^0(z) &= \sum_{i,j,k} (z_i z_j z_k + z_i^* z_j^* z_k^*), \\ \mathcal{H}_3^1(z) &= \sum_{i,j,k} (z_i z_j z_k^* + z_i^* z_j^* z_k), \end{aligned} \quad (25)$$

...

are all manifestly real and fulfill the required conditions. We number this family of cost functions  $\{\mathcal{H}_k^0, \mathcal{H}_k^1, \dots, \mathcal{H}_k^{\lfloor k/2 \rfloor}\}$  and refer to them collectively as *Wirtinger potentials* for  $\mathcal{H}$ , with  $\mathcal{H}_k^p$  referred to as the  $p$ -potential of order  $k$  for  $\mathcal{H}$ . Here  $p$  refers to the number of conjugate terms in the leading product of each conjugate pair. For instance, each pair of  $\mathcal{H}_4^1(z)$  has the form  $z_i z_j z_k z_l^* + z_i^* z_j^* z_k^* z_l$ , while  $\mathcal{H}_4^2(z)$  conjugate pairs have the form  $z_i z_j z_k^* z_l^* + z_i^* z_j^* z_k z_l$ . A general definition for Wirtinger potentials of arbitrary order can be found in Appendix C. Each  $\mathcal{H}_k^p$  is real-valued and has identical values for  $z \in \mathbb{C}^n$ , preserving Property 1. So too are properly scaled linear combinations of  $\mathcal{H}_k^p$ , including the special case  $\mathcal{H}_k^C = \frac{1}{\lfloor k/2 \rfloor} \sum_p \mathcal{H}_k^p$ .

Wirtinger potentials enable flexibility in modeling oscillator

systems while maintaining consistency with the Ising paradigm. For example, in a 3-SAT problem, the optimization target comprises three types of terms: linear, quadratic, and cubic (corresponding to  $k = 1, 2,$  and  $3,$  respectively). This means that multiple oscillator modeling options exist for each type of term. The energy function Eq. 15 is one such option, and our empirical evaluations indicate that this combination delivers the best performance in our benchmarks. However, it may not be the optimal choice for all problem types. In the following section (IV C), we discuss a real case that leverages the variety of these models to achieve effective binarization for oscillator-based Ising machines. A thorough analysis of higher-order systems would require extensive theoretical and experimental study, which is beyond the scope of this work. Future research may explore these formulations to further enhance the capabilities of oscillator-based Ising machines.

### C. Binarization Behavior: Quadratic Problems

Recall that reading out solutions to QUBO problems from OIMs requires converting each oscillator's continuous phase (from  $0$  to  $2\pi$ ) into discrete Ising spins ( $+1$  or  $-1$ ). Two (somewhat independent) factors can impact the final results: ① the state of the oscillators just prior to the readout and ② the actual readout process:

1. **The state:** At the end of annealing, depending on the governing dynamics, the oscillators can strongly binarize or not. Clearly, a strongly binarized system (Fig. 3-c or d) is more robust to classification error than a weakly binarized system (Fig. 3-a or b).
2. **The readout:** Mathematically, the readout step can be represented as introducing a binarization axis  $\vec{b}$ , which separates oscillators into two groups by their phases. For convenience, we can treat  $\vec{b}$  as the imaginary axis with the associated binarization function  $f_B(z) = \text{sign}(\text{Re}(z))$ . This axis may or may not be the binarization axis  $\vec{b}$  corresponding to the lowest energy assignment, depending on the phase relationship between the oscillators and the readout circuit, leading to four cases illustrated in Fig. 3.

Our Wirtinger potentials have implications for both factors as we explore next.

Whether  $\vec{b} = \vec{b}$  depends on the problem formulation. Consider a quadratic Hamiltonian  $\mathcal{H}(s_1, s_2) = s_1 s_2$ .  $\mathcal{H}$  has three main Wirtinger potentials, the 0-potential  $\mathcal{H}_2^0(z_1, z_2)$ , the 1-potential  $\mathcal{H}_2^1(z_1, z_2)$ , and their convex combinations, including the ‘‘complete’’ C-potential  $\mathcal{H}_2^C(z_1, z_2)$ . Their explicit forms are given by

$$\begin{aligned} \mathcal{H}_2^0(z_1, z_2) &= z_1 z_2 + z_1^* z_2^* \\ \mathcal{H}_2^1(z_1, z_2) &= z_1^* z_2 + z_1 z_2^* \\ \mathcal{H}_2^C(z_1, z_2) &= 0.5(z_1 z_2 + z_1^* z_2^*) \\ &\quad + 0.5(z_1^* z_2 + z_1 z_2^*). \end{aligned} \quad (26)$$

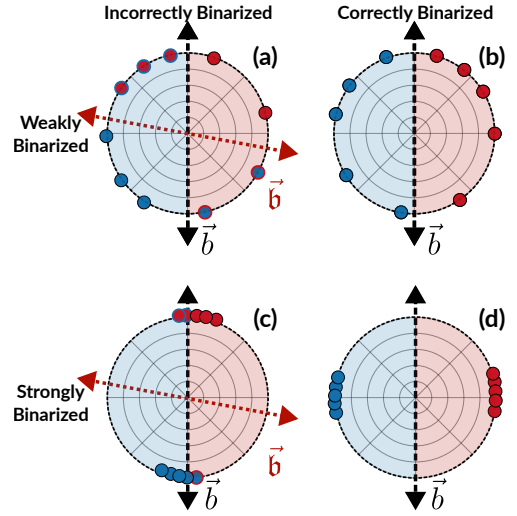


FIG. 3. Example phase plots, where a system can either be strongly/weakly binarized (which corresponds the variance of the phase distribution) and correctly/incorrectly binarized (which corresponds to classification errors from axis misalignment).

Each potential gives identical values at  $z_1, z_2 \in \{|z|e^{i0}, |z|e^{i\pi}\}$  (typical binarization reference points). However, they do not behave identically under phase translations. Consider a global phase offset  $\phi$ . The 1-potential remains invariant, as

$$\begin{aligned} \mathcal{H}_2^1(e^{i\phi} z_1, e^{i\phi} z_2) &= e^{i(\phi-\phi)} z_1^* z_2 + e^{i(\phi-\phi)} z_1 z_2^* \\ &= z_1^* z_2 + z_1 z_2^* = \mathcal{H}_2^1(z_1, z_2). \end{aligned} \quad (27)$$

The same is not true, however, of the 0-potential or C-potential, where

$$\begin{aligned} \mathcal{H}_2^0(e^{i\phi} z_1, e^{i\phi} z_2) &= e^{i2\phi} z_1 z_2 + e^{-i2\phi} z_1^* z_2^* \\ &\neq \mathcal{H}_2^0(z_1, z_2) \end{aligned} \quad (28)$$

and

$$\begin{aligned} \mathcal{H}_2^C(e^{i\phi} z_1, e^{i\phi} z_2) &= 0.5e^{i2\phi} z_1 z_2 + 0.5e^{-i2\phi} z_1^* z_2^* \\ &\quad + 0.5(z_1^* z_2 + z_1 z_2^*) \\ &\neq \mathcal{H}_2^C(z_1, z_2) \end{aligned} \quad (29)$$

in general. For instance, for  $z_1 = e^{i0}, z_2 = e^{i\pi}, \phi = \pi/3$ , we have

$$\begin{aligned} \mathcal{H}_2^0(e^{i\phi} z_1, e^{i\phi} z_2) &= \frac{1}{2} [\cos(\pi + \pi/3) + \cos(\pi - \pi/3)] \\ &= -0.5 \neq -1.0 = \mathcal{H}_2^0(z_1, z_2). \end{aligned} \quad (30)$$

Investigating the Hessians provides more context. For convenience, we assume that the local dynamics confine each oscillator to unit amplitude, allowing for a phase-reduced model

$$\begin{aligned} \mathcal{H}_2^0(\theta_1, \theta_2) &= \cos(\theta_1 + \theta_2) \\ \mathcal{H}_2^1(\theta_1, \theta_2) &= \cos(\theta_1 - \theta_2) \\ \mathcal{H}_2^C(\theta_1, \theta_2) &= \frac{1}{2} \cos(\theta_1 - \theta_2) + \frac{1}{2} \cos(\theta_1 + \theta_2) \end{aligned} \quad (31)$$

with Hessians

$$\begin{aligned}\nabla^2 \mathcal{H}_2^0(\theta_1, \theta_2) &= \begin{bmatrix} -\cos(\theta_1 + \theta_2) & -\cos(\theta_1 + \theta_2) \\ -\cos(\theta_1 + \theta_2) & -\cos(\theta_1 + \theta_2) \end{bmatrix} \\ \nabla^2 \mathcal{H}_2^1(\theta_1, \theta_2) &= \begin{bmatrix} -\cos(\theta_1 - \theta_2) & \cos(\theta_1 - \theta_2) \\ \cos(\theta_1 - \theta_2) & -\cos(\theta_1 - \theta_2) \end{bmatrix} \\ \nabla^2 \mathcal{H}_2^C(\theta_1, \theta_2) &= \frac{1}{2} \nabla^2 \mathcal{H}_2^0(\theta_1, \theta_2) + \frac{1}{2} \nabla^2 \mathcal{H}_2^1(\theta_1, \theta_2)\end{aligned}\quad (32)$$

by the linearity of the Hessian operator.

$\nabla^2 \mathcal{H}_2^1(\theta_1, \theta_2)$  and  $\nabla^2 \mathcal{H}_2^0(\theta_1, \theta_2)$  have eigenvalues  $\{0, 2\}$ , however their null spaces  $\mathcal{N}$  are disjoint. Specifically,  $\mathcal{N}(\nabla^2 \mathcal{H}_2^0) = \text{Span}\{(1, -1)^\top\}$ ,  $\mathcal{N}(\nabla^2 \mathcal{H}_2^1) = \text{Span}\{(1, 1)^\top\}$ . In other words, the 1-potential has zero curvature along the  $(1, 1)^\top$  vector while being strongly convex along  $(1, -1)$ . In contrast, the 0-potential is strongly convex along  $(1, 1)^\top$  while having zero curvature along  $(1, -1)$ . Neither potential is strongly convex in the neighborhood of their fixed points, causing each to have an uncountable number of solutions.

However, the convex combination  $\nabla^2 \mathcal{H}_2^C(\theta_1, \theta_2)$  is full-rank and positive definite in the neighborhood of all  $\{0, \pi\}$  minima, meaning it guarantees descent to the unique phase minimizer within each neighborhood.

SHIL performs a similar function, adding the diagonal matrix

$$\nabla^2 \mathcal{H}_2^{\text{SHIL}} = 2 \begin{bmatrix} \cos(2\theta_1) & 0 \\ 0 & \cos(2\theta_2) \end{bmatrix}, \quad (33)$$

which makes  $\nabla^2 \{\mathcal{H}_2^1 + \mathcal{H}_2^{\text{SHIL}}\}$  full rank and positive definite in the neighborhood of  $\{0, \pi\}$ . Therefore, we have two options for binarizing quadratic Hamiltonians:

1. Add  $\mathcal{H}_2^{\text{SHIL}}$  to the problem Hamiltonian.
2. Use  $\mathcal{H}_2^C(z_1, z_2)$ .

Option 1 is typical in OIM literature [56, 98]. However, our analysis offers an alternative.  $\mathcal{H}_2^C(z_1, z_2)$  or, more generally, a convex combination of the 1-potential  $\mathcal{H}_2^1(z_1, z_2)$  and the 0-potential  $\mathcal{H}_2^0(z_1, z_2)$  creates a strongly convex function in the neighborhood of  $\{0, \pi\}$  fixed points. In the next section, we explore this possibility to induce binarization in 3-SAT problems while maintaining high-quality solutions.

#### D. Binarization Behavior: SAT Problems

Similar to the quadratic case, there are multiple choices to formulate a cubic oscillator model. Our empirical analysis on 3-SAT problems shows that the model defined by Eq. 15 attains the highest solution quality, but only weakly binarizes. Conversely, replacing the terms in Eq. 15 with the complete form in Eq. 24 yields a new energy function which strongly binarizes but suffers from inferior optimization performance. In our experiments, this variant solved 61.8%, 17%, 2%, and 0% of the instances for the uf-50, uf-75, uf-100, and uf-150 benchmarks, respectively, based on 100 independent trials per instance, which is similar to the baseline we compared with. This trade-off motivates the question: Can we design an oscillator network that simultaneously (i) achieves high

solution quality, (ii) respects the Ising Hamiltonian, and (iii) yields binary spin values at convergence?

To address this, we examine the contributions of each term in the formulation Eq. 15 independently. Linear and cubic terms inherently attain weak binarization, as their Hessians have non-zero curvature along  $(1)^\top$ ,  $(1, 1, 1)^\top$ . The primary difference between the Hamiltonians lies with the quadratic terms. As we showed in the previous subsection, C-potential quadratic Hamiltonians are strongly convex in the vicinity of  $\{0, \pi\}$  phase points, promoting strong binarization. In contrast, the 1-potential does not binarize, as the system is invariant to global phase shifts.

Therefore, introducing a time-varying quadratic Wirtinger potential can provide a strong binarization force while preserving the optimization performance of the oscillator network. More specifically, we can get a model with a stronger binarization tendency by selecting  $\mathcal{H}_2^C$  for the quadratic terms as follows:

$$\begin{aligned}\mathcal{H}'' &= \frac{1}{2} \sum_{i=1}^n h_i(z_i + z_i^*) \\ &+ \frac{1}{4} \sum_{i=1}^n \sum_{j=1}^n J_{ij} (2z_i z_j^* + z_i z_j + z_i^* z_j^*) \\ &+ \frac{1}{2} \left( \sum_{i=1}^n \sum_{j=1}^n \sum_{k=1}^n P_{ijk} z_i z_j z_k^* \right. \\ &\left. + \sum_{i=1}^n \sum_{j=1}^n \sum_{k=1}^n P_{ijk} z_i z_j^* z_k^* \right) + \text{constant}.\end{aligned}\quad (34)$$

It is important to note that after binarization, both Hamiltonian Eq. 15 and Eq. 34, as well as any combination of them, yield identical values to the discrete Ising formulation, although binarization introduces a slight modification in the energy landscape. To demonstrate the effectiveness of our binarization strategies, we evaluated four scenarios on 45 uf100-430 3-SAT instances:

- **None:** The system evolves under Hamiltonian Eq. 15.
- **Static Potential:** The system evolves under Hamiltonian Eq. 34.
- **Annealed SHIL:** The system uses Hamiltonian Eq. 15 augmented with a SHIL signal, where the coefficient increases linearly.
- **Annealed Potential:** The system starts with Hamiltonian Eq. 15 and linearly transitions to Hamiltonian Eq. 34 to achieve binarization.

Fig. 4 presents the distribution of the final oscillator phases. In the *None* scenario (a), the distributions are weakly peaked at 0 and  $\pi$ . However, a significant proportion of the phases are spread between the peaks, indicating little inherent binarization. In contrast, the SHIL, Static, and Annealed strategies (b)–(d) exhibit a strong binarization tendency.

Fig. 5 shows the cumulative final energy distribution of each binarization strategy. The distributions represent 45 problems from uf100-430 ( $n = 100$ ,  $m = 430$ ), each with 100 runs.

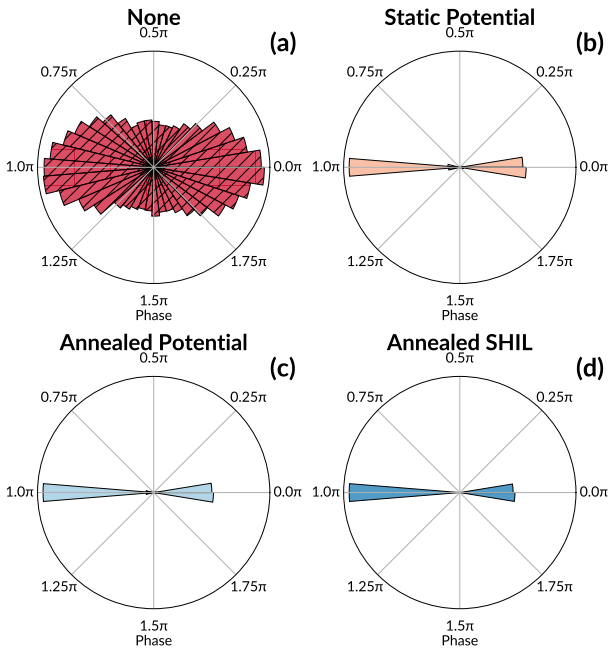


FIG. 4. Polar histograms of phase values for the different binarization strategies discussed.

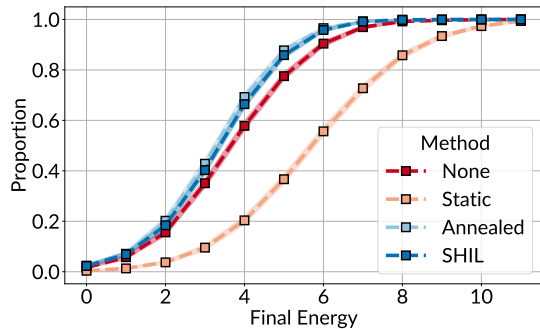


FIG. 5. Cumulative distribution of final energy values for the different binarization strategies discussed. Each line represents the distribution of 45 problems from `uf100-430` with 100 trials each. 99% confidence intervals are provided as shaded lines around each estimate, however they are typically too narrow to be visible.

We use bootstrap resampling with  $10^4$  resamples to obtain 99% confidence intervals (shaded area around lines); however, in most cases, they are too narrow to be easily visible.

In lieu of final energy, a narrower figure of merit (FoM) should be just the probability of reaching the ground state (energy=0). However, we note that these are stochastic results, and one way to better see through the underlying reality is to see the distribution of all solutions. (Another way is to show the narrow FoM over more test benchmarks.) In the cumulative distribution, the higher the curve, the better. As we can see, the SHIL and Annealed strategies deliver performance that is similar to or slightly better than that achieved by the system evolving under Hamiltonian Eq. 15 alone. We hypothesize that the induced binarization acts as a form of stochastic perturbation,

which may help the system escape local minima during the optimization process.

## V. DISCUSSION

Phase reduction approaches, including the Kuramoto model, fail to capture the full dynamics of oscillator-based Ising machines in real-world applications. We present a comprehensive Hopf oscillator model that explicitly incorporates amplitude dynamics, addressing this fundamental limitation. Compared to the existing baseline, our model defines a clear energy function with corresponding dynamics and achieves better performance.

Our study focuses on the theoretical soundness of phase–amplitude models for oscillator-based Ising machines. Recent studies [52, 89, 105] demonstrate that integrating heuristic mechanisms substantially improve Ising-machine-based 3-SAT solver performance. Our model enhancements establish a solid foundation for these advances.

Incorporating amplitude dynamics introduces an additional degree of freedom. The use of a complex oscillator representation paves another way for further research. We interpret the local dynamics term  $f(z_i)$  in the oscillator model (Eq. 12) not only as a mechanism to preserve physical oscillator properties but also as a means to improve the performance of the oscillator-based Ising machine. Here, we provide a perspective for future studies: oscillator-based Ising machines rely on binarization and nonlinearity to achieve better performance on MAX-CUT problems [56, 93], whereas Linear Ising Machines (LIMs) like BRIM [35] do not. By engineering the local dynamics, one can steer the oscillator-based Ising machine to mimic the dynamics of LIMs. For example, in quadratic MAX-CUT problems, the oscillator dynamics  $f(z_i)$  could be designed to preserve the real part of the oscillator representation  $z_i$  while adjusting the imaginary part to maintain essential oscillator properties. This approach shifts the optimization focus from system-level strategies to tuning inherent oscillator properties, although further experimental validation remains necessary.

## VI. CONCLUSION

Our work is driven by the need for a more accurate model for oscillator-based Ising machines. We observed several fundamental inconsistencies in existing phase-amplitude models. By addressing these issues, we propose a model that incorporates both phase and amplitude dynamics, features a physically meaningful Lyapunov function, and remains compatible with the widely used phase-only models in oscillator-based Ising machine implementations. Experiments show that our model outperforms existing phase-amplitude approaches in optimization performance and exhibits a correct energy minimization tendency.

Our phase-amplitude model provides a more faithful framework for modeling oscillator-based Ising machines when amplitude dynamics cannot be neglected. This includes spintronic oscillators that naturally exhibit coupled amplitude

and phase dynamics, NEMS oscillators operating in regimes where amplitude variations are significant, and emerging photonic systems. By providing a rigorous mathematical foundation that captures these dynamics, our model enables more accurate simulations and predictions of system behavior, which is crucial for the design and optimization of OIMs. Accurate modeling further enhances practical applications, including portfolio optimization, drug discovery, wireless communication, and a wide range of other combinatorial optimization problems.

Furthermore, we propose a method to generalize the model for constructing higher-order Ising machines and an implementable approach for extracting solutions from the oscillators. These findings contribute to both the theoretical understanding and practical realization of oscillator-based Ising machines, offering valuable directions for future research and development in this promising field.

### ACKNOWLEDGMENTS

This work was supported in part by NSF under Awards No. 2231036 and No. 2233378, and by DARPA under contract No. FA8650-23-C-7312.

### DATA AVAILABILITY

The data that support the findings of this article are openly available [106].

### APPENDIX

#### A. Example: Mapping a 3-SAT problem to Ising Hamiltonian

We illustrate the mapping on the single clause

$$C = (x_1 \vee \neg x_2 \vee x_3).$$

Our goal is to construct a Hamiltonian  $H_C$  for this clause. When  $H_C$  is minimized to 0, the clause is satisfied; otherwise, it contributes 1 to the total energy.

**Mapping Method:** Each Boolean  $x_i \in \{0, 1\}$  is represented by an Ising spin  $s_i \in \{+1, -1\}$ , with

$$s_i = +1 \iff x_i = \text{true}, \quad s_i = -1 \iff x_i = \text{false}.$$

**Step 1: Literal energy terms.** For each literal  $\ell$ , define

$$f(\ell) = \begin{cases} 1 - s_i, & \ell = x_i, \\ 1 + s_i, & \ell = \neg x_i. \end{cases}$$

In our clause,

$$f(x_1) = 1 - s_1, \quad f(\neg x_2) = 1 + s_2, \quad f(x_3) = 1 - s_3,$$

according to the mapping method,  $f(\ell) = 0$  when the literal is true, and  $f(\ell) = 2$  otherwise.

**Step 2: Clause energy by multiplication.** To ensure the energy is nonzero only when all three literals fail, we take the product:

$$(1 - s_1)(1 + s_2)(1 - s_3) = \begin{cases} 0, & \text{if at least one literal is true,} \\ 8, & \text{if all three literals are false.} \end{cases}$$

**Step 3: Normalization.** Dividing by 8 yields the clause Hamiltonian

$$H_C = \frac{(1 - s_1)(1 + s_2)(1 - s_3)}{8} = \begin{cases} 0, & \text{clause satisfied,} \\ 1, & \text{clause unsatisfied.} \end{cases}$$

Finally, for a full 3-SAT problem with clauses  $C_1, \dots, C_M$ , we sum these terms:

$$\mathcal{H} = \sum_{j=1}^M H_{C_j},$$

so  $\mathcal{H}$  counts exactly the number of unsatisfied clauses.

#### B. Wirtinger Calculus for Non-Holomorphic Hamiltonians

Let  $z = x + iy$  be a complex  $n$ -dimensional vector, where  $x, y \in \mathbb{R}^n$ . When the Hamiltonian  $\mathcal{H}$  depends on both  $z = x + iy$  and its complex conjugate  $z^* = x - iy$ , it is typically not holomorphic and the usual derivative does not exist. Wirtinger calculus treats  $z$  and  $z^*$  as independent variables. For any real-valued  $\mathcal{H}(z, z^*)$ , Wirtinger partial derivatives are defined as

$$\frac{\partial \mathcal{H}}{\partial z_i} \triangleq \frac{1}{2} \left( \frac{\partial \mathcal{H}}{\partial x_i} - i \frac{\partial \mathcal{H}}{\partial y_i} \right),$$

$$\frac{\partial \mathcal{H}}{\partial z_i^*} \triangleq \frac{1}{2} \left( \frac{\partial \mathcal{H}}{\partial x_i} + i \frac{\partial \mathcal{H}}{\partial y_i} \right).$$

As a consequence of the definitions above, we have

$$\frac{\partial \mathcal{H}}{\partial z_i} = \left( \frac{\partial \mathcal{H}}{\partial z_i^*} \right)^*$$

$$\frac{\partial \mathcal{H}}{\partial z_i^*} = \left( \frac{\partial \mathcal{H}}{\partial z_i} \right)^*.$$

While the formal definitions are expressed using  $x$  and  $y$ , the Wirtinger partial derivatives behave as expected for a function defined in terms of  $z$  and  $z^*$ . For example, one can easily verify that  $\frac{\partial}{\partial z}[zz^*] = z^*$  and  $\frac{\partial}{\partial z^*}[zz^*] = z$ .

Additionally, a function  $\mathcal{H}$  is holomorphic if and only if  $\partial \mathcal{H} / \partial z_i^* = 0$  for all  $z_i$ . Intuitively, Wirtinger calculus treats  $\mathcal{H}$  as a function over  $\mathbb{R}^{2n}$  instead of  $\mathbb{C}^n$ , using appropriately defined isomorphisms to transform between  $\mathcal{H}(x, y) : \mathbb{R}^{2n} \rightarrow \mathbb{R}$ ,  $\mathcal{H}(z, z^*) : \mathbb{C}^{2n} \rightarrow \mathbb{R}$  and  $\mathcal{H}(z) : \mathbb{C}^n \rightarrow \mathbb{R}$ . From this perspective, typical objects from multivariate calculus

(gradients, Hessians, ...) have a natural extension to real-valued, non-holomorphic functions. Additional details can be found in the excellent introduction to the subject by Kreutz-Delgado [73]. Crucial for our purposes is the definition of the Wirtinger gradient

$$\nabla_z \mathcal{H} \triangleq \left( \frac{\partial \mathcal{H}}{\partial z} \right)^\dagger,$$

where  $\frac{\partial \mathcal{H}}{\partial z} \in \mathbb{C}^{2n}$  is the vector

$$\left( \frac{\partial \mathcal{H}}{\partial z_1}, \dots, \frac{\partial \mathcal{H}}{\partial z_n}, \frac{\partial \mathcal{H}}{\partial z_1^*}, \dots, \frac{\partial \mathcal{H}}{\partial z_n^*} \right)^\top$$

and  $(\cdot)^\dagger$  denotes a conjugate transpose. Since Wirtinger partials have the bijective relationship  $\frac{\partial \mathcal{H}}{\partial z_\ell} = \left( \frac{\partial \mathcal{H}}{\partial z_\ell^*} \right)^*$ , we focus only on the non-conjugated components.

**Example:** Consider an energy function  $\mathcal{H}(z, z^*) = z z^*$ . Treating  $z^*$  as constant when differentiating with respect to  $z$  (and vice versa), we obtain

$$\frac{\partial \mathcal{H}}{\partial z} = z^*, \quad \frac{\partial \mathcal{H}}{\partial z^*} = z.$$

Since  $\partial \mathcal{H} / \partial z^* = z \neq 0$ ,  $\mathcal{H}$  is non-holomorphic.

**Energy Minimization via Gradient Descent:** For a real-valued Hamiltonian  $\mathcal{H}(z, z^*)$ , a small update  $\Delta z$  produces

$$\Delta \mathcal{H} \approx \frac{\partial \mathcal{H}}{\partial z} \Delta z + \frac{\partial \mathcal{H}}{\partial z^*} \Delta z^*.$$

Recall that  $\frac{\partial \mathcal{H}}{\partial z^*} = \left( \frac{\partial \mathcal{H}}{\partial z} \right)^*$  and vice versa. Therefore, to minimize  $\Delta \mathcal{H}$ , it suffices to choose

$$\Delta z \propto - \frac{\partial \mathcal{H}}{\partial z^*} \quad (\text{B1})$$

which produces

$$\Delta \mathcal{H} \propto -2 \left\| \frac{\partial \mathcal{H}}{\partial z^*} \right\|^2.$$

Choosing a “step size” of  $\eta$ , we therefore have a well-defined gradient descent scheme:

$$z^{k+1} \leftarrow z^k - \eta \frac{\partial \mathcal{H}}{\partial z^*}.$$

In the previous example  $\partial \mathcal{H} / \partial z^* = z$ , so iterating  $z^{k+1} \leftarrow z^k - \eta z^k$  drives  $z \rightarrow 0$ , the minimizer of the energy  $\mathcal{H} = |z|^2$ .

### C. General PUBO Wirtinger Potentials

As defined in Sec. III B, we can express the “complete”  $k^{\text{th}}$  order PUBO Hamiltonian  $\mathcal{H}_k^C : \mathbb{C}^n \rightarrow \mathbb{R}$  as

$$\mathcal{H}_k^C(z) = \frac{1}{\lfloor k/2 \rfloor} \sum_{p=1}^{\lfloor k/2 \rfloor} \mathcal{H}_k^p(z),$$

where each  $p$ -potential has  $m_p = 2 \binom{k}{p}$  terms and each  $\mathcal{H}_k^p : \mathbb{C}^n \rightarrow \mathbb{R}$  has the form

$$\begin{aligned} \mathcal{H}_k^p(z) = & \frac{1}{2^k} \sum_{j=1}^{m_p} c_{p,j} \left( y_{p,j}^{(1)} \cdots y_{p,j}^{(p)} (y_{p,j}^{(p+1)})^* \cdots (y_{p,j}^{(k)})^* \right. \\ & \left. + (y_{p,j}^{(1)})^* \cdots (y_{p,j}^{(p)})^* y_{p,j}^{(p+1)} \cdots y_{p,j}^{(k)} \right), \end{aligned}$$

where  $p$  denotes the number of non-conjugated terms in the first product and each term  $y_{p,j}^{(q)}$  refers to some complex variable  $z_\ell$  appearing as the  $q^{\text{th}}$  term in the  $j^{\text{th}}$  product.

- 
- [1] Kotaro Tanahashi, Shinichi Takayanagi, Tomomitsu Motohashi, and Shu Tanaka. Application of ising machines and a software development for ising machines. *Journal of the Physical Society of Japan*, 88(6):061010, 2019.
  - [2] Matthieu Parizy, Przemyslaw Sadowski, and Nozomu Togawa. Cardinality constrained portfolio optimization on an ising machine. In *2022 IEEE 35th International System-on-Chip Conference (SOCC)*, pages 1–6. IEEE, 2022.
  - [3] Zetian Mao, Yoshiki Matsuda, Ryo Tamura, and Koji Tsuda. Chemical design with gpu-based ising machines. *Digital Discovery*, 2(4):1098–1103, 2023.
  - [4] Siya Bao, Masashi Tawada, Shu Tanaka, and Nozomu Togawa. An ising-machine-based solver of vehicle routing problem with balanced pick-up. *IEEE Transactions on Consumer Electronics*, 2023.
  - [5] Yui Tsuyumine, Kenichi Masuda, Takeshi Hachikawa, Tsuyoshi Haga, Yuta Yachi, Tatsuhiko Shirai, Masashi Tawada, and Nozomu Togawa. Optimization of practical time-dependent vehicle routing problem by ising machines. In *2024 IEEE International Conference on Consumer Electronics (ICCE)*, pages 1–5. IEEE, 2024.
  - [6] Utkarsh Azad, Bikash K Behera, Emad A Ahmed, Prasanta K Panigrahi, and Ahmed Farouk. Solving vehicle routing problem using quantum approximate optimization algorithm. *IEEE Transactions on Intelligent Transportation Systems*, 24(7):7564–7573, 2022.
  - [7] Jonas Stein, Daniëlle Schuman, Magdalena Benkard, Thomas Holger, Wanja Sajko, Michael Kölle, Jonas Nüßlein, Leo Sünkel, Olivier Salomon, and Claudia Linnhoff-Popien. Exploring unsupervised anomaly detection with quantum boltzmann machines in fraud detection. *arXiv preprint arXiv:2306.04998*, 2023.

- 2023.
- [8] Nasa Matsumoto, Yohei Hamakawa, Kosuke Tatsumura, and Kazue Kudo. Distance-based clustering using qubo formulations. *Scientific reports*, 12(1):2669, 2022.
  - [9] Kenta Kirihara, Hidetaka Imai, Eisuke Kuroda, Jun Yamazaki, and Akiko Masaki-Kato. Exploring potential applications of ising machines for power system operations. *IEEE Access*, 11:68004–68017, 2023.
  - [10] Abhishek Kumar Singh, Kyle Jamieson, Peter L McMahon, and Davide Venturelli. Ising machines’ dynamics and regularization for near-optimal mimo detection. *IEEE Transactions on Wireless Communications*, 21(12):11080–11094, 2022.
  - [11] Shreesha Sreedhara, Jaijeet Roychowdhury, Joachim Wabnig, and Pavan Koteswar Srinath. Mu-mimo detection using oscillator ising machines. In *2023 IEEE/ACM International Conference on Computer Aided Design (ICCAD)*, pages 1–9. IEEE, 2023.
  - [12] Eliahu Cohen, Maya Carmi, Ron Heiman, Ofer Hadar, and Asaf Cohen. Image restoration via ising theory and automatic noise estimation. In *2013 IEEE International Symposium on Broadband Multimedia Systems and Broadcasting (BMSB)*, pages 1–5, 2013.
  - [13] Shaila Niazi, Shuvro Chowdhury, Navid Anjum Aadit, Masoud Mohseni, Yao Qin, and Kerem Y Camsari. Training deep boltzmann networks with sparse ising machines. *Nature Electronics*, pages 1–10, 2024.
  - [14] Chunshu Wu, Ruibing Song, Chuan Liu, Yunan Yang, Ang Li, Michael Huang, and Tong Geng. Extending power of nature from binary to real-valued graph learning in real world. In *The Twelfth International Conference on Learning Representations*, 2024.
  - [15] Ruibing Song, Chunshu Wu, Chuan Liu, Ang Li, Michael Huang, and Tony Tong Geng. Ds-gl: Advancing graph learning via harnessing nature’s power within scalable dynamical systems. In *2024 ACM/IEEE 51st Annual International Symposium on Computer Architecture (ISCA)*, pages 45–57. IEEE, 2024.
  - [16] Chuan Liu, Ruibing Song, Chunshu Wu, Pouya Haghi, and Tong Geng. Instatrain: Adaptive training via ultra-fast natural annealing within dynamical systems. In *The Thirteenth International Conference on Learning Representations*, 2025.
  - [17] Chuan Liu, Chunshu Wu, Ruibing Song, Ang Li, Ying Nian Wu, and Tong Geng. An expressive and self-adaptive dynamical system for efficient function learning. In *Forty-second International Conference on Machine Learning*, 2025.
  - [18] Mark W Johnson, Mohammad HS Amin, Suzanne Gildert, Trevor Lanting, Firas Hamze, Neil Dickson, Richard Harris, Andrew J Berkley, Jan Johansson, Paul Bunyk, et al. Quantum annealing with manufactured spins. *Nature*, 473(7346):194–198, 2011.
  - [19] Andrew D King, Jack Raymond, Trevor Lanting, Richard Harris, Alex Zucca, Fabio Altomare, Andrew J Berkley, Kelly Boothby, Sara Ejtemaee, Colin Enderud, et al. Quantum critical dynamics in a 5,000-qubit programmable spin glass. *Nature*, 617(7959):61–66, 2023.
  - [20] William R Clements, Jelmer J Renema, Y Henry Wen, Helen M Chrzanoski, W Steven Kolthammer, and Ian A Walmsley. Gaussian optical ising machines. *Physical Review A*, 96(4):043850, 2017.
  - [21] D Pierangeli, G Marcucci, and C Conti. Large-scale photonic ising machine by spatial light modulation. *Physical review letters*, 122(21):213902, 2019.
  - [22] Alireza Marandi, Zhe Wang, Kenta Takata, Robert L Byer, and Yoshihisa Yamamoto. Network of time-multiplexed optical parametric oscillators as a coherent ising machine. *Nature Photonics*, 8(12):937–942, 2014.
  - [23] Bo Wu, Wenkai Zhang, Shiji Zhang, Hailong Zhou, Zhichao Ruan, Ming Li, Dongmei Huang, Jianji Dong, and Xinliang Zhang. A monolithically integrated optical ising machine. *Nature Communications*, 16(1):1–11, 2025.
  - [24] Marcello Calvanese Strinati, Davide Pierangeli, and Claudio Conti. All-optical scalable spatial coherent ising machine. *Physical Review Applied*, 16(5):054022, 2021.
  - [25] Zhe Wang, Alireza Marandi, Kai Wen, Robert L Byer, and Yoshihisa Yamamoto. Coherent ising machine based on degenerate optical parametric oscillators. *Physical Review A*, 88(6):063853, 2013.
  - [26] Qizhuang Cen, Hao Ding, Tengfei Hao, Shanhong Guan, Zhiqiang Qin, Jiaming Lyu, Wei Li, Ninghua Zhu, Kun Xu, Yitang Dai, et al. Large-scale coherent ising machine based on optoelectronic parametric oscillator. *Light: Science & Applications*, 11(1):333, 2022.
  - [27] Yuan Gao, Guanyu Chen, Luo Qi, Wujie Fu, Zifeng Yuan, and Aaron J Danner. Photonic ising machines for combinatorial optimization problems. *Applied Physics Reviews*, 11(4), 2024.
  - [28] Davide Pierangeli, Giulia Marcucci, Daniel Brunner, and Claudio Conti. Noise-enhanced spatial-photonic ising machine. *Nanophotonics*, 9(13):4109–4116, 2020.
  - [29] Wenchen Sun, Wenjia Zhang, Yuanyuan Liu, Qingwen Liu, and Zuyuan He. Quadrature photonic spatial ising machine. *Optics Letters*, 47(6):1498–1501, 2022.
  - [30] Takashi Takemoto, Masato Hayashi, Chihiro Yoshimura, and Masanao Yamaoka. A  $2 \times 30k$ -spin multi-chip scalable cmos annealing processor based on a processing-in-memory approach for solving large-scale combinatorial optimization problems. *IEEE Journal of Solid-State Circuits*, 55(1):145–156, 2019.
  - [31] Satoshi Matsubara, Motomu Takatsu, Toshiyuki Miyazawa, Takayuki Shibasaki, Yasuhiro Watanabe, Kazuya Takemoto, and Hirotaka Tamura. Digital annealer for high-speed solving of combinatorial optimization problems and its applications. In *2020 25th Asia and South Pacific Design Automation Conference (ASP-DAC)*, pages 667–672. IEEE, 2020.
  - [32] Francesco Belletti, Maria Cotallo, Andrés Cruz, Luis Antonio Fernandez, Antonio Gordillo-Guerrero, Marco Guidetti, Andrea Maiorano, Filippo Mantovani, Enzo Marinari, Victor Martin-Mayor, et al. Janus: An fpga-based system for high-performance scientific computing. *Computing in Science & Engineering*, 11(1):48–58, 2008.
  - [33] Marco Baity-Jesi, Rachel A Baños, Andres Cruz, Luis Antonio Fernandez, José Miguel Gil-Narvi6n, Antonio Gordillo-Guerrero, David Iniguez, Andrea Maiorano, Filippo Mantovani, Enzo Marinari, et al. Janus ii: A new generation application-driven computer for spin-system simulations. *Computer Physics Communications*, 185(2):550–559, 2014.
  - [34] Masanao Yamaoka, Chihiro Yoshimura, Masato Hayashi, Takuya Okuyama, Hidetaka Aoki, and Hiroyuki Mizuno. A 20k-spin ising chip to solve combinatorial optimization problems with cmos annealing. *IEEE Journal of Solid-State Circuits*, 51(1):303–309, 2015.
  - [35] Richard Afoakwa, Yiqiao Zhang, Uday Kumar Reddy Vengalam, Zeljko Ignjatovic, and Michael Huang. BRIM: Bistable Resistively-Coupled Ising Machine. In *2021 IEEE International Symposium on High-Performance Computer Architecture (HPCA)*, pages 749–760, Seoul, Korea (South), February 2021. IEEE.
  - [36] Yuqi Su, Tony Tae-Hyoung Kim, and Bongjin Kim. Flexspin: A cmos ising machine with 256 flexible spin processing elements with 8-b coefficients for solving combinatorial optimization

- problems. *IEEE Journal of Solid-State Circuits*, 59(8):2659–2670, 2024.
- [37] Shanshan Xie, Siddhartha Raman Sundara Raman, Can Ni, Meizhi Wang, Mengtian Yang, and Jaydeep P Kulkarni. Ising-cim: A reconfigurable and scalable compute within memory analog ising accelerator for solving combinatorial optimization problems. *IEEE Journal of Solid-State Circuits*, 57(11):3453–3465, 2022.
- [38] Toshimori Honjo, Tomohiro Sonobe, Kensuke Inaba, Takahiro Inagaki, Takuya Ikuta, Yasuhiro Yamada, Takushi Kazama, Koji Enbutsu, Takeshi Umeki, Ryoichi Kasahara, et al. 100,000-spin coherent ising machine. *Science advances*, 7(40):eabh0952, 2021.
- [39] Artem Litvinenko, Roman Khymyn, Victor H González, Roman Ovcharov, Ahmad A Awad, Vasyl Tyberkevych, Andrei Slavin, and Johan Åkerman. A spinwave ising machine. *Communications Physics*, 6(1):227, 2023.
- [40] Wenshuo Yue, Teng Zhang, Zhaokun Jing, Kai Wu, Yuxiang Yang, Zhen Yang, Yongqin Wu, Weihai Bu, Kai Zheng, Jin Kang, et al. A scalable universal ising machine based on interaction-centric storage and compute-in-memory. *Nature Electronics*, 7(10):904–913, 2024.
- [41] Xi Chen, Dongliang Yang, Geunwoo Hwang, Yujiao Dong, Binbin Cui, Dingchen Wang, Hegan Chen, Ning Lin, Wenqi Zhang, Huihan Li, et al. Oscillatory neural network-based ising machine using 2d memristors. *ACS nano*, 18(16):10758–10767, 2024.
- [42] Olivier Maher, Manuel Jiménez, Corentin Delacour, Nele Harnack, Juan Núñez, María J Avedillo, Bernabé Linares-Barranco, Aida Todri-Sanial, Giacomo Indiveri, and Siegfried Karg. A cmos-compatible oscillation-based vo2 ising machine solver. *Nature Communications*, 15(1):3334, 2024.
- [43] Jia Si, Shuhan Yang, Yunuo Cen, Jiaer Chen, Yingna Huang, Zhaoyang Yao, Dong-Jun Kim, Kaiming Cai, Jerald Yoo, Xuanyao Fong, et al. Energy-efficient superparamagnetic ising machine and its application to traveling salesman problems. *Nature Communications*, 15(1):3457, 2024.
- [44] Zihao Chen, Zhili Xiao, Mahmoud Akl, Johannes Leugring, Omowuyi Olajide, Adil Malik, Nik Dennler, Chad Harper, Subhankar Bose, Hector A Gonzalez, et al. On-off neuromorphic ising machines using fowler-nordheim annealers. *Nature communications*, 16(1):3086, 2025.
- [45] Andrew Lucas. Ising formulations of many NP problems. *Frontiers in Physics*, 2, 2014.
- [46] V. Kolmogorov and R. Zabih. What energy functions can be minimized via graph cuts? *IEEE Transactions on Pattern Analysis and Machine Intelligence*, 26(2):147–159, February 2004.
- [47] D. Freedman and P. Drineas. Energy Minimization via Graph Cuts: Settling What is Possible. In *2005 IEEE Computer Society Conference on Computer Vision and Pattern Recognition (CVPR’05)*, volume 2, pages 939–946, San Diego, CA, USA, 2005. IEEE.
- [48] Martin Anthony, Endre Boros, Yves Crama, and Aritanan Gruber. Quadratic reformulations of nonlinear binary optimization problems. *Mathematical Programming*, 162(1-2):115–144, March 2017.
- [49] Hüsrev Cilasun, Ziqing Zeng, Ramprasath S, Abhimanyu Kumar, Hao Lo, William Cho, William Moy, Chris H. Kim, Ulya R. Karpuzcu, and Sachin S. Sapatnekar. 3SAT on an all-to-all-connected CMOS Ising solver chip. *Scientific Reports*, 14(1):10757, May 2024.
- [50] Dmitrii Dobrynin, Adrien Renaudineau, Mohammad Hizzani, Dmitrii Strukov, Masoud Mohseni, and John Paul Strachan. Energy landscapes of combinatorial optimization in Ising machines. *Physical Review E*, 110(4):045308, October 2024.
- [51] Connor Bybee, Denis Kleyko, Dmitri E. Nikonov, Amir Khosrowshahi, Bruno A. Olshausen, and Friedrich T. Sommer. Efficient optimization with higher-order Ising machines. *Nature Communications*, 14(1):6033, September 2023.
- [52] Anshujit Sharma, Matthew Burns, Andrew Hahn, and Michael Huang. Augmenting an electronic Ising machine to effectively solve boolean satisfiability. *Scientific Reports*, 13(1):22858, December 2023.
- [53] Taro Kanao and Hayato Goto. Simulated bifurcation for higher-order cost functions. *Applied Physics Express*, 16(1):014501, January 2023.
- [54] Mohammad Khairul Bashar and Nikhil Shukla. Designing Ising machines with higher order spin interactions and their application in solving combinatorial optimization. *Scientific Reports*, 13(1):9558, June 2023.
- [55] Yoshiki Kuramoto. Self-entrainment of a population of coupled non-linear oscillators. In Huzihiro Araki, editor, *International Symposium on Mathematical Problems in Theoretical Physics*, pages 420–422, Berlin, Heidelberg, 1975. Springer.
- [56] Tianshi Wang and Jaijeet Roychowdhury. OIM: Oscillator-based Ising Machines for Solving Combinatorial Optimisation Problems, March 2019. arXiv:1903.07163 [cs].
- [57] Mohammad Khairul Bashar, Antik Mallick, Daniel S. Truesdell, Benton H. Calhoun, Siddharth Joshi, and Nikhil Shukla. Experimental Demonstration of a Reconfigurable Coupled Oscillator Platform to Solve the Max-Cut Problem. *IEEE Journal on Exploratory Solid-State Computational Devices and Circuits*, 6(2):116–121, December 2020.
- [58] Sourav Dutta, Abhishek Khanna, and Suman Datta. Understanding the Continuous-Time Dynamics of Phase-Transition Nano-Oscillator-Based Ising Hamiltonian Solver. *IEEE Journal on Exploratory Solid-State Computational Devices and Circuits*, 6(2):155–163, December 2020.
- [59] Antik Mallick, Mohammad Khairul Bashar, Daniel S. Truesdell, Benton H. Calhoun, Siddharth Joshi, and Nikhil Shukla. Using synchronized oscillators to compute the maximum independent set. *Nature Communications*, 11(1):4689, September 2020.
- [60] Ibrahim Ahmed, Po-Wei Chiu, and Chris H. Kim. A Probabilistic Self-Annealing Compute Fabric Based on 560 Hexagonally Coupled Ring Oscillators for Solving Combinatorial Optimization Problems. In *2020 IEEE Symposium on VLSI Circuits*, pages 1–2, Honolulu, HI, USA, June 2020. IEEE.
- [61] Jeffrey Chou, Suraj Bramhavar, Siddhartha Ghosh, and William Herzog. Analog Coupled Oscillator Based Weighted Ising Machine. *Scientific Reports*, 9(1):14786, October 2019.
- [62] Markus Graber and Klaus Hofmann. Firefly: A versatile experimental platform for oscillator-based ising machines. *IEEE Transactions on Circuits and Systems I: Regular Papers*, 2024.
- [63] Shreesha Sreedhara and Jaijeet Roychowdhury. A novel oscillator ising machine coupling scheme for high-quality optimization. In *International Conference on Unconventional Computation and Natural Computation*, pages 203–218. Springer, 2024.
- [64] Neha Garg, Sanyam Singhal, Aniket Sadashiva, Pranaba K Muduli, and Debanjan Bhowmik. Phase-binarized dipole-coupled spin hall nano oscillators (shnos) as ising machines. In *2024 IEEE 24th International Conference on Nanotechnology (NANO)*, pages 196–200. IEEE, 2024.
- [65] Karlheinz Ochs, Bakr Al Beattie, and Sebastian Jenderny. An ising machine solving max-cut problems based on the circuit synthesis of the phase dynamics of a modified kuramoto model.

- In *2021 IEEE International Midwest Symposium on Circuits and Systems (MWSCAS)*, pages 982–985. IEEE, 2021.
- [66] Shreesha Sreedhara, Jaijeet Roychowdhury, Joachim Wabnig, and Pavan Srinath. Digital emulation of oscillator ising machines. In *2023 Design, Automation & Test in Europe Conference & Exhibition (DATE)*, pages 1–2. IEEE, 2023.
- [67] Hüseyin Cilasun, William Moy, Ziqing Zeng, Tahmida Islam, Hao Lo, Alex Vanasse, Megan Tan, Mohammad Anees, Abhimanyu Kumar, Sachin S Sapatnekar, et al. A coupled-oscillator-based ising chip for combinatorial optimization. *Nature Electronics*, pages 1–10, 2025.
- [68] Matthew H Matheny, Jeffrey Emenheiser, Warren Fon, Airlie Chapman, Anastasiya Salova, Martin Rohden, Jarvis Li, Mathias Hudoba de Badyn, Márton Pósfai, Leonardo Duenas-Osorio, et al. Exotic states in a simple network of nanoelectromechanical oscillators. *Science*, 363(6431):eaav7932, 2019.
- [69] Andrei Slavina and Vasil Tiberkevich. Nonlinear auto-oscillator theory of microwave generation by spin-polarized current. *IEEE Transactions on Magnetics*, 45(4):1875–1918, 2009.
- [70] Lucia Valentina Gambuzza, Jesus Gómez-Gardeñes, and Mattia Frasca. Amplitude dynamics favors synchronization in complex networks. *Scientific reports*, 6(1):24915, 2016.
- [71] Neha Garg, Sanyam Singhal, Nakul Aggarwal, Aniket Sadashiva, Pranaba K Muduli, and Debanjan Bhowmik. Improved time complexity for spintronic oscillator ising machines compared to a popular classical optimization algorithm for the max-cut problem. *Nanotechnology*, 35(46):465201, 2024.
- [72] Dmitri E Nikonov, Gyorgy Csaba, Wolfgang Porod, Tadashi Shibata, Danny Voils, Dan Hammerstrom, Ian A Young, and George I Bourianoff. Coupled-oscillator associative memory array operation for pattern recognition. *IEEE Journal on Exploratory Solid-State Computational Devices and Circuits*, 1:85–93, 2015.
- [73] Ken Kreutz-Delgado. The Complex Gradient Operator and the CR-Calculus, June 2009. arXiv:0906.4835 [math].
- [74] Taro Kanao and Hayato Goto. High-accuracy ising machine using kerr-nonlinear parametric oscillators with local four-body interactions. *npj Quantum Information*, 7(1), January 2021.
- [75] Liam Quinn, Yiqing Xu, Julien Fatome, Gian-Luca Oppo, Stuart G. Murdoch, Miro Erkintalo, and Stéphane Coen. Coherent ising machine based on polarization symmetry breaking in a driven kerr resonator, 2024.
- [76] S. F. Edwards and P. W. Anderson. Theory of spin glasses. *Journal of Physics F: Metal Physics*, 5(5):965, May 1975.
- [77] David Sherrington and Scott Kirkpatrick. Solvable Model of a Spin-Glass. *Physical Review Letters*, 35(26):1792–1796, December 1975. Publisher: American Physical Society.
- [78] Ernst Ising. Beitrag zur theorie des ferromagnetismus. *Zeitschrift für Physik*, 31(1):253–258, 1925.
- [79] F Barahona. On the computational complexity of Ising spin glass models. *Journal of Physics A: Mathematical and General*, 15(10):3241–3253, October 1982.
- [80] Sorin Istrail. Statistical mechanics, three-dimensionality and NP-completeness: I. Universality of intracatability for the partition function of the Ising model across non-planar surfaces (extended abstract). In *Proceedings of the Thirty-Second Annual ACM Symposium on Theory of Computing, STOC '00*, pages 87–96, New York, NY, USA, May 2000. Association for Computing Machinery.
- [81] Naeimeh Mohseni, Peter L. McMahon, and Tim Byrnes. Ising machines as hardware solvers of combinatorial optimization problems. *Nature Reviews Physics*, 4(6):363–379, June 2022. Number: 6 Publisher: Nature Publishing Group.
- [82] J. E. Beasley. OR-Library: Distributing Test Problems by Electronic Mail. *Journal of the Operational Research Society*, 41(11):1069–1072, November 1990. Publisher: Taylor & Francis \_eprint: <https://doi.org/10.1057/jors.1990.166>.
- [83] Maliheh Aramon, Gili Rosenberg, Elisabetta Valiante, Toshiyuki Miyazawa, Hirotaka Tamura, and Helmut G. Katzgraber. Physics-Inspired Optimization for Quadratic Unconstrained Problems Using a Digital Annealer. *Frontiers in Physics*, 7, 2019.
- [84] Hayato Goto, Kotaro Endo, Masaru Suzuki, Yoshisato Sakai, Taro Kanao, Yohei Hamakawa, Ryo Hidaka, Masaya Yamasaki, and Kosuke Tatsumura. High-performance combinatorial optimization based on classical mechanics. *Science Advances*, 7(6):eabe7953, February 2021. Publisher: American Association for the Advancement of Science.
- [85] Atanu Rajak, Sei Suzuki, Amit Dutta, and Bikas K Chakrabarti. Quantum annealing: an overview. *Philosophical Transactions of the Royal Society A*, 381(2241):20210417, 2023. Publisher: The Royal Society.
- [86] Takahiro Inagaki, Yoshitaka Haribara, Koji Igarashi, Tomohiro Sonobe, Shuhei Tamate, Toshimori Honjo, Alireza Marandi, Peter L. McMahon, Takeshi Umeki, Koji Enbutsu, Osamu Tadanaga, Hirokazu Takenouchi, Kazuyuki Aihara, Ken-ichi Kawarabayashi, Kyo Inoue, Shoko Utsunomiya, and Hiroki Takesue. A coherent Ising machine for 2000-node optimization problems. *Science*, 354(6312):603–606, November 2016. Publisher: American Association for the Advancement of Science.
- [87] Mohammad Hizzani, Arne Heitmann, George Hutchinson, Dmitrii Dobrynin, Thomas Van Vaerenbergh, Tinis Bhattacharya, Adrien Renaudineau, Dmitri Strukov, and John Paul Strachan. Memristor-based hardware and algorithms for higher-order Hopfield optimization solver outperforming quadratic Ising machines. In *2024 IEEE International Symposium on Circuits and Systems (ISCAS)*, pages 1–5, May 2024. ISSN: 2158-1525.
- [88] Toshimori Honjo, Tomohiro Sonobe, Kensuke Inaba, Takahiro Inagaki, Takuya Ikuta, Yasuhiro Yamada, Takushi Kazama, Koji Enbutsu, Takeshi Umeki, Ryoichi Kasahara, Ken-ichi Kawarabayashi, and Hiroki Takesue. 100,000-spin coherent Ising machine. *Science Advances*, 7(40):eabh0952, September 2021. Publisher: American Association for the Advancement of Science.
- [89] Anshujit Sharma, Matthew Burns, and Michael C. Huang. Combining Cubic Dynamical Solvers with Make/Break Heuristics to Solve SAT. *LIPICs, Volume 271, SAT 2023*, 271:25:1–25:21, 2023. Artwork Size: 21 pages, 4440368 bytes ISBN: 9783959772860 Medium: application/pdf Publisher: Schloss Dagstuhl – Leibniz-Zentrum für Informatik.
- [90] Michael Sipser. *Introduction to the Theory of Computation*. Cengage Learning, Australia Brazil Japan Korea Mexico Singapore Spain United Kingdom United States, 3rd edition edition, June 2012.
- [91] Stefano Gherardini, Shamik Gupta, and Stefano Ruffo. Spontaneous synchronisation and nonequilibrium statistical mechanics of coupled phase oscillators. *Contemporary Physics*, 59(3):229–250, July 2018. Publisher: Taylor & Francis \_eprint: <https://doi.org/10.1080/00107514.2018.1464100>.
- [92] Bastian Pietras and Andreas Daffertshofer. Network dynamics of coupled oscillators and phase reduction techniques. *Physics Reports*, 819:1–105, July 2019.
- [93] Jaykumar Vaidya, R. S. Surya Kanthi, and Nikhil Shukla. Creating electronic oscillator-based Ising machines without

- external injection locking. *Scientific Reports*, 12(1):981, January 2022. Number: 1 Publisher: Nature Publishing Group.
- [94] Tingting Zhang, Qichao Tao, Bailiang Liu, Andrea Grimaldi, Eleonora Raimondo, Manuel Jiménez, María José Avedillo, Juan Nuñez, Bernabé Linares-Barranco, Teresa Serrano-Gotarredona, Giovanni Finocchio, and Jie Han. A Review of Ising Machines Implemented in Conventional and Emerging Technologies. *IEEE Transactions on Nanotechnology*, 23:704–717, 2024.
- [95] Aleksandr Mikhailovich Lyapunov. The general problem of the stability of motion. *International journal of control*, 55(3):531–534, 1992.
- [96] Hao Lo, William Moy, Hanzhao Yu, Sachin Sapatnekar, and Chris H. Kim. An Ising solver chip based on coupled ring oscillators with a 48-node all-to-all connected array architecture. *Nature Electronics*, 6(10):771–778, October 2023. Publisher: Nature Publishing Group.
- [97] William Moy, Ibrahim Ahmed, Po-wei Chiu, John Moy, Sachin S. Sapatnekar, and Chris H. Kim. A 1,968-node coupled ring oscillator circuit for combinatorial optimization problem solving. *Nature Electronics*, 5(5):310–317, May 2022. Publisher: Nature Publishing Group.
- [98] Olivier Maher, Manuel Jiménez, Corentin Delacour, Nele Harnack, Juan Nuñez, María J. Avedillo, Bernabé Linares-Barranco, Aida Todri-Sanial, Giacomo Indiveri, and Siegfried Karg. A CMOS-compatible oscillation-based VO2 Ising machine solver. *Nature Communications*, 15(1):3334, April 2024. Publisher: Nature Publishing Group.
- [99] Olivier Maher, Roy Bernini, Nele Harnack, Bernd Gotsmann, Marilyne Sousa, Valeria Bragaglia, and Siegfried Karg. Highly reproducible and CMOS-compatible VO2-based oscillators for brain-inspired computing. *Scientific Reports*, 14(1):11600, May 2024. Publisher: Nature Publishing Group.
- [100] S. Dutta, A. Khanna, A. S. Assoa, H. Paik, D. G. Schlom, Z. Toroczkai, A. Raychowdhury, and S. Datta. An Ising Hamiltonian solver based on coupled stochastic phase-transition nano-oscillators. *Nature Electronics*, 4(7):502–512, July 2021. Publisher: Nature Publishing Group.
- [101] Andrea Grimaldi, Luciano Mazza, Eleonora Raimondo, Pietro Tullo, Davi Rodrigues, Kerem Y. Camsari, Vincenza Crupi, Mario Carpentieri, Vito Puliafito, and Giovanni Finocchio. Evaluating Spintronics-Compatible Implementations of Ising Machines. *Physical Review Applied*, 20(2):024005, August 2023. Publisher: American Physical Society.
- [102] Jia Si, Shuhan Yang, Yunuo Cen, Jiaer Chen, Yingna Huang, Zhaoyang Yao, Dong-Jun Kim, Kaiming Cai, Jerald Yoo, Xuanyao Fong, and Hyunsoo Yang. Energy-efficient superparamagnetic Ising machine and its application to traveling salesman problems. *Nature Communications*, 15(1):3457, April 2024.
- [103] Holger H Hoos and Thomas Stützle. SATLIB: An Online Resource for Research on SAT. *Kluwer Academic Publishers*, 2000.
- [104] Rémi Monasson, Riccardo Zecchina, Scott Kirkpatrick, Bart Selman, and Lidror Troyansky. Determining computational complexity from characteristic ‘phase transitions’. *Nature*, 400(6740):133–137, 1999.
- [105] Ahmet Yusuf Salim, Bart Selman, Henry Kautz, Zeljko Ignjatovic, and Selçuk Köse. SKI-SAT: A CMOS-compatible Hardware for Solving SAT Problems, November 2024. arXiv:2411.01028 [cs].
- [106] ACAL. oscillator-paper-data. <https://github.com/ur-acal/prapplied-oscillator-data>.